

# Graphene Oxide-Silver Nanocomposite Induced Apoptosis in Human Hepatoma (HepG2) Cells Through Oxidative Stress and Caspase Dependent Signalling Pathway

Neelima Sharma<sup>a</sup>, Surajit Mondal<sup>a</sup>, Hari Om Yadav<sup>b</sup>, & Rishi Sharma<sup>c\*</sup>

<sup>a</sup>Department of Pharmaceutical Sciences and Technology Birla Institute of Technology, Mesra, Ranchi 835 215, India

<sup>b</sup>Council of Scientific & Industrial Research, New Delhi 110 001, India

<sup>c</sup>Department of Physics, Birla Institute of Technology, Mesra, Ranchi 835 215, India

*Received: 14 May 2021 & Accepted: 30 November 2022*

At present, the nanotechnology-based therapeutic agents have been emerged as the most reliable tool for various dangerous disorders including cancer. Liver cancer is one of the top five deadliest cancers. Hepatocellular Carcinoma (HCC) is the third most leading cause of death after lung and stomach cancer. Graphene Oxide, due to its unique chemical, mechanical, and optical properties, has offered a wide range of applications in biomedical fields. Silver nanoparticles can easily enter into mammalian cells, accumulate in the macrophages, and interact with biological molecules. In the present investigation, the effects of Graphene Oxide-Ag nanocomposites on human Hepatoma Cells (HepG2) have been investigated. Graphene oxide has been synthesised by modified Hummer's method and further, Graphene Oxide-Ag nanocomposites have been prepared. The effect of nanoparticles on cell viability has been observed. For understanding the molecular pathway, the effects on oxidative stress (ROS and GSH levels), Caspase-3 Activity and Apoptotic Cell Population have been examined. Further, to confirm the role of oxidative stress and caspase-3 activity, the cell viability has been measured in the presence or absence of specific inhibitors. The results demonstrate that GO-Ag nanocomposites induce cytotoxicity, oxidative stress and apoptosis in HepG2 cells through caspase dependent pathway. The oxidative stress plays a crucial role in GO-Ag nanocomposites induced caspase dependent apoptosis. Thus, it can be concluded that GO-Ag nanocomposites show therapeutic efficacy in cancer cells.

**Keywords:** Apoptosis, Caspase, Graphene oxide, Nanocomposite, Oxidative stress

## 1 Introduction

Nanotechnology is a new scientific system for management, development and synthesis of atomic or molecular substances. The next generation of tools to cure various diseases including cancer is assumed to be nano-science-based antioxidants and therapeutic agents<sup>1</sup>. Graphene has risen as the brilliant material and wonderful star among the various nanomaterials reported to date. Graphene is an atomically dense, two-dimensional (2-D) layer of sp<sup>2</sup> bonded carbon atoms arranged in a framework of honeycomb<sup>2</sup>. Graphene which is an advanced material that has appeared as a rapid rising star in material science, consists of one-atom-thick planar layer composed of sp<sup>2</sup>-bonded carbon structure of an extraordinarily high crystal and electronic quality<sup>3</sup>. Graphene and its derivatives offer a range of nano-therapeutic modalities for phototherapy, drug delivery, and combination therapy related to its unique mechanical, chemical and optical properties. Graphene Oxide

(GO), a graphene equivalent is obtained through the chemical treatment of graphite by subsequent water dispersion, oxidation or appropriate organic solvents. GO contains significant numbers of oxygen functional groups such as, hydroxyl, carbonyl, carboxyl and epoxy groups on its basal plane and edges<sup>4</sup>. Graphene Oxide causes cytotoxicity by disruption to the plasma membrane, alteration in reactive oxygen species (ROS) level and damage to DNA in different cells.

Due to astonishing bio-medical properties of silver nanoparticles, these are also recommended as a part of the treatment against cancer. Silver nanoparticles have applications as targeted drugs as these can easily enter in mammalian cells, concentrate in the macrophage, and can induce toxicity due to interaction with biological molecules<sup>5</sup>. Considering the advantages of combination therapy, targeted drug delivery (nano-carriers) based on nanoparticles (NP) have been designed to increase drug accumulation at tumour sites to enhance permeability and retention pharmacokinetic profiles and reduce side effects. Consequently, the development of a chemotherapeutic

\*Corresponding author (E-mail: rishisharmabit@hotmail.com)

agent and chemo sensitizer using nano-carriers has been suggested as a novel and promising cancer treatment strategy<sup>6</sup>.

Cancer, a general term for a range of diseases, is an unexpected and uncontrolled cell proliferation known as a "malignant neoplasm". In the developed countries, it is the main cause of deaths and the second in developing countries. Liver cancer is the one of the top five deadliest cancers, however, hepatocellular carcinoma is the most mutual histological subtype<sup>7, 8</sup>. Hepatocellular carcinoma (HCC) is one of the most widespread cancers and has become the 3<sup>rd</sup> foremost cause of cancer death after lung cancer and stomach cancer<sup>9</sup>. Nevertheless, most anticancer drugs are causing high toxicity and low specificity, which show systemic toxicity and severe side effects.

Nanomaterials are used to diagnose as well as treat cancers<sup>10</sup>. Recently, polymeric nanoparticles and nanocomposites have been enlisted as promising anticancer drug carriers. These can also be used as a targeted drug delivery system that helps to increase therapeutic properties and reduce adverse effects on normal organs<sup>11</sup>. Therefore, the aim of present investigation is to determine the effect of Graphene oxide- silver nanocomposites on human hepatoma cells (HepG2) under in-vitro conditions and its molecular aspect.

## 2 Materials and Methods

### 2.1 Reagents and chemicals

All the chemicals used in this study were of highest-grade purity available. 3(4, 5-dimethyl-2-yl) 2, 5 diphenyl tetrazolium bromide (MTT), O-phthalaldehyde (OPT), dithiothreitol (DTT), DEVD-AFC substrate, 2, 7 dichlorofluoresce in diacetate (DCFH DA) were purchased from Sigma-Aldrich (St. Louis, MO). Fetal bovine serum (FBS), trichloroacetic acid (TCA), triton- $\times$ 100, dithiothreitol (DTT), Dulbecco's modified eagle's medium (DMEM), antibioticantimycotic solution were purchased from Himedia Laboratories Ltd. (Mumbai, India).

### 2.2 Synthesis of graphene oxide- silver nanocomposites (GO-Ag Nanocomposites)

Graphene Oxide was synthesized simply using a solution-based process by improved Hummer's method<sup>12</sup>. In this method, GO was prepared by the oxidation of natural graphite powder by adding concentrated H<sub>2</sub>SO<sub>4</sub> under stirring in an ice bath. Under vigorous agitation, KMnO<sub>4</sub> was added slowly

and the reaction system was transferred to a 40°C on oil bath and vigorously stirred for about 0.5 h. Then, water was added and the solution was stirred for 15 min at 95°C. Additional, water was added and followed by a slow addition of H<sub>2</sub>O<sub>2</sub> turning the color of the solution from dark brown to yellow. The mixture was filtered and washed with 1:10 HCl aqueous solution to remove metal ions. The resulting solid was dried in air and diluted to make a graphite oxide aqueous dispersion. Finally, it was purified by dialysis for one week by using a dialysis membrane to remove the remaining metal species. The resultant graphite oxide aqueous dispersion was then diluted and stirred overnight. After that it was sonicated for 30 min to exfoliate it to GO.

Further, for the preparation of GO-Ag Nanocomposite, 4 ml of AgNO<sub>3</sub> solution (0.2 M) was added to 20 ml of GO dispersion. (1 mg/ml) and stirred magnetically at 800 rpm for 3 h at 25 °C. Then, 2 ml of ascorbic acid solution (0.5 M) was quickly added to the mixed solution, and the mixture was maintained under vigorous magnetic stirring at 1200 rpm for 1 h. The reaction product was separated by centrifugation by 7000 rpm for 10 mins and washed repeatedly with ultrapure water until it was free of impurities. Finally, the nanocomposite was dispersed in 20 ml of ultrapure water<sup>13</sup>.

### 2.3 Characterization of GO-Ag nanocomposites

The synthesized GO-Ag nanocomposites were characterized using Fourier Transform Infrared (FTIR) Spectroscopy (SHIMADZU IR Prestige-21, Japan), XRD(Rigaku, Smart Lab 9kW), Scanning Electron Microscopy (SEM) (JEOL JSM 6390LV, USA) and Raman Spectroscopy (in Via Reflex Raman Spectrometer, Renishaw, U.K.).

### 2.4 Cell culture

Human hepatoma cell line (HepG2) was procured from National Centre for Cell Sciences (Pune, India), having 70–80% confluency. The procured cells were centrifuged and cultured in Dulbecco's modified eagle's medium (DMEM) supplemented with 10% fetal bovine serum, 100  $\mu$ g / ml streptomycin and 100 U/ml penicillin at 37 °C with 5% CO<sub>2</sub> supply in humidified incubator. The cell density was adjusted to  $\sim 1.5 \times 10^6$  cells/ ml for all the further experiments.

### 2.5 Cell viability assay

The colorimetric MTT assay was performed to determine the viability of HepG2Cells<sup>14</sup>. Tetrazolium salt reduction is generally recognized as effective

method to analyse cell proliferation. The yellow tetrazolium MTT (3-(4, 5-dimethylthiazol-2-yl)-2, 5-diphenyltetrazolium bromide) is reduced by the action of dehydrogenase enzyme of metabolically active cells. For MTT assay, the cells were seeded in a 96 well plate at a concentration of  $1.0 \times 10^4$  cells per well. Different concentrations of GO-Ag nanocomposite (1, 10, 25, 50 and 100  $\mu\text{g}/\text{ml}$ ) were added and incubated with 5 %  $\text{CO}_2$  at  $37^\circ\text{C}$  for 18 h. 10  $\mu\text{L}$  MTT (5 mg / mL) was added to each well for 4h, the plate was centrifuged and supernatant was decanted. Further, formazan crystals were dissolved by adding 100  $\mu\text{L}$  DMSO to each well. The absorbance in a micro titer plate reader was measured at 570 nm (Thermo Scientific). As a result of the MTT assay, three concentration of GO-Ag nanocomposite (25, 50 and 100  $\mu\text{g}/\text{ml}$ ) were chosen for further investigation.

#### 2.6 Reactive oxygen species (ROS) measurement

The cell concentration was adjusted to  $1.5 \times 10^6$  cells / ml and 200  $\mu\text{l}$  of cell suspension was plated to each well. GO-Ag nanocomposite concentrations (10, 25, 50  $\mu\text{g}/\text{ml}$ ), and 2  $\mu\text{l}$  of 2, 7 dichlorofluorescein diacetate (DCFH DA) (100  $\mu\text{M}$ ) were added simultaneously for 1, 3 and 6 hours. After incubation, the cells were re-suspended in PBS and resulting fluorescence was measured at 480 nm and 530 nm respectively for excitation and emission wavelength<sup>15</sup>.

#### 2.7 Glutathione level

HepG2 cells were treated with different concentrations of GO-Ag nanocomposites (10, 25 and 50  $\mu\text{g}/\text{ml}$ ) for 1, 3, 6 h. The incubated cells were re-suspended in 100  $\mu\text{l}$  phosphate EDTA buffer and sonicated for 10 min. Further, trichloroacetic acid (100  $\mu\text{l}$ ) was added and incubated for 10 min on ice. The supernatant of cells was collected after centrifugation and 10  $\mu\text{l}$  of O-phthalaldehyde (1 mg/mL) was added. The resulting intensity of fluorescence was measured at the excitation (390 nm) and emission wavelength (470 nm)<sup>16</sup>.

#### 2.8 Caspase-3 activity

The cells (a population of  $3.0 \times 10^6$  cells/ml) were treated with GO-Ag nanocomposite (10, 25 and 50  $\mu\text{g}/\text{ml}$ ) and incubated for 6 hours. Treated cells were re-suspended in 50  $\mu\text{l}$  lysis buffer and incubated for 10 mins on ice. The supernatant was collected and further incubated at  $37^\circ\text{C}$  for 2 h after adding reaction buffer (50  $\mu\text{l}$ ) and DEVD-AFC (5  $\mu\text{l}$ , final concentration 50  $\mu\text{M}$ ). The

subsequent fluorescent was measured at an excitation (400 nm) and an emission wavelength (505 nm)<sup>17</sup>.

#### 2.9 Cell cycle study

HepG2 Cells ( $1.5 \times 10^6$  cells/ml) were treated with different concentrations of GO-Ag nanocomposite (10, 25 and 50  $\mu\text{g}/\text{ml}$ ) for 18 hours. The cells were collected, washed with PBS and fixed by drop by drop addition of 70 % ice-cold ethanol. The fixed cells were suspended in 1 ml PBS after washing. Phosphate citrate buffer was added and the cells were incubated for 60 mins at room temperature. The cells were centrifuged, re-suspended in 0.5 ml of PI stain and 0.5 ml RNase A (50 g/ml) and further incubated for 30 mins in dark. The fluorescence of the PI was measured using a FL-2 filter (585 nm) with a flow cytometer<sup>18</sup>.

#### 2.10 Statistical analysis

The results are expressed as mean  $\pm$  Standard Deviation (SD). Statistical evaluation has been done by using the software Graph pad prism version 8.4.2 according to one-way ANOVA.

### 3 Results and Discussion

#### 3.1 Characterization

FTIR spectroscopy is generally used for the analysis of various functional groups in the samples. FTIR spectra of GO-Ag nanocomposites were shown in Fig. 1. The intense and broad peak that centred at  $3400\text{ cm}^{-1}$  confirmed the presence of O-H bond (hydroxyl group). C=O stretching (–COOH group) was presented at  $1736\text{ cm}^{-1}$  and peaks between  $1015\text{ cm}^{-1}$  and  $1250\text{ cm}^{-1}$  were due to C-O-C stretching (epoxy group). The sharp peak found at  $1625\text{ cm}^{-1}$  was a resonance peak that could be assigned to the stretching and bending vibration of OH groups of water molecules adsorbed on graphene oxide. The peak at  $1380\text{ cm}^{-1}$  raised from C-H bending<sup>19</sup>. This FTIR spectra confirmed the synthesis of Graphene oxide.

The XRD pattern of prepared GO and its nanocomposites were shown in Fig. 2. The diffraction pattern illustrating one diffraction peak centred around  $2\theta = 9.8$ , indicated the formation of GO. While in XRD pattern of GO-Ag Nanocomposites, the peaks obtained at  $2\theta$  values were centred around 38 degree and 44 degree which matched with the reported peaks<sup>20,21</sup>.

Raman Spectroscopy is a potent technique to reveal the structural changes in graphene upon functionalization. The intensity ratio of D to G band (ID/IG) is used as a measure of the degree of crystallization in graphene sheets<sup>22</sup>. In the present

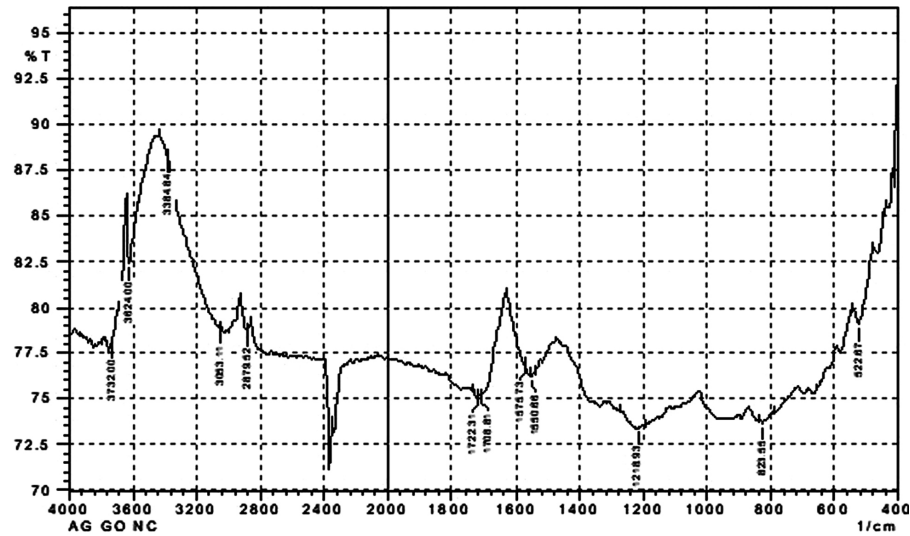


Fig. 1 — FTIR of graphene oxide silver nano-composite.

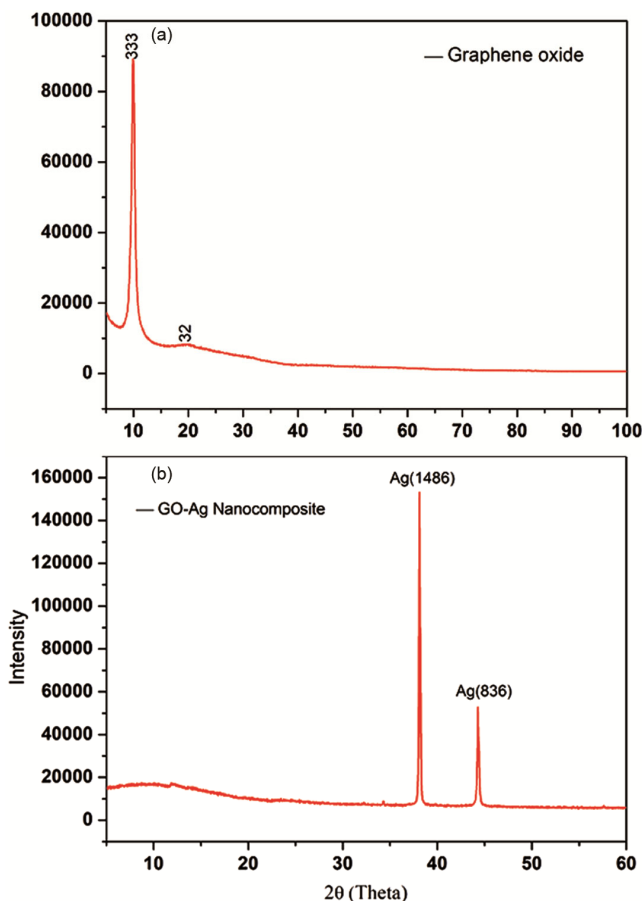


Fig. 2 — XRD of Graphene Oxide and Graphene Oxide- Silver nanocomposite.

investigation, GO showed its characteristic D peak and G peak around  $1350\text{ cm}^{-1}$  and  $1601\text{ cm}^{-1}$  respectively, which indicated  $\text{sp}^2$ -hybridized carbon atoms stretch. The ID/IG ratio was found to be 0.84.

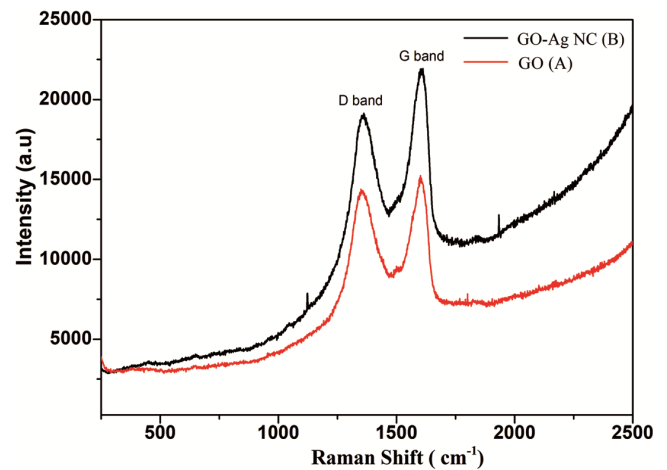


Fig. 3 — Raman spectroscopy of (a) Graphene oxide and (b) Graphene oxide Silver nanocomposite.

The synthesized GO-Ag nanocomposites also showed similar kind of peaks, D peak and G peak around  $1363\text{ cm}^{-1}$  and  $1560\text{ cm}^{-1}$  respectively. The observed ID/IG ratio of GO-Ag Nanocomposites was 0.88 which was higher than GO. The increased ID/IG ratio indicated the embellishment of nanoparticles on GO sheets (Fig. 3)<sup>23</sup>. After doping, the D and G band values were increased due to intercalation of AgNPs on the GO surface.

The FESEM images of the GO and GO-Ag nanocomposites were shown in Fig. 4. All the observations had been recorded at 100000 X magnification. The morphology of the graphene and its derivatives mainly depends on the process of their synthesis. The FESEM image of GO revealed a two-dimensional sheet-like structure consisting of multiple lamellar layers and rich wrinkled structures on the

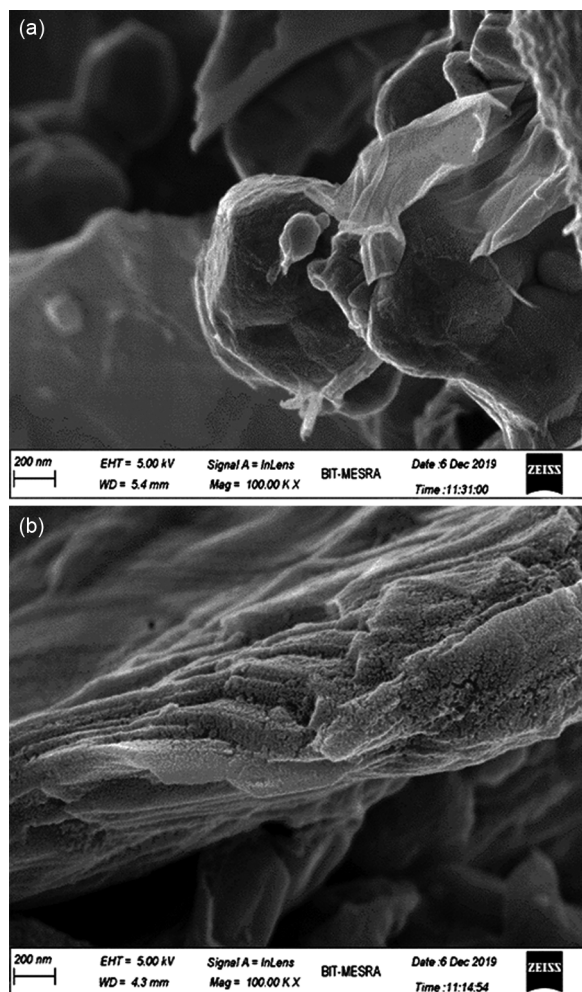


Fig. 4 — (a) FESEM of Graphene oxide, and (b) Graphene oxide Silver nanocomposite.

surface<sup>24</sup>. It had been observed from Fig. 4b that the layered structure of GO had been ruptured after mixing with Ag. This also confirmed the formation of GO-Ag nano-composites. All these characterization results confirmed that GO-Ag nanocomposites had been synthesized successfully.

### 3.2 Effect of graphene oxide silver nanocomposite on cell viability

The cell viability resultsshowed that there was a concentration- dependent significant decrease in cell viability of Hep G2 cells with increasing concentrations of GO-Ag nanocomposites. At 50  $\mu\text{g/ml}$  concentration, the % cell viability was approx. 65 % which showed anti-cancer property of GO-Ag nanocomposites (Fig. 5). The result with 100  $\mu\text{g/ml}$  concentration was almost similar, thus, 3 effective concentrations (10, 25 and 50  $\mu\text{g/ml}$ ) had been selected for further parameters.

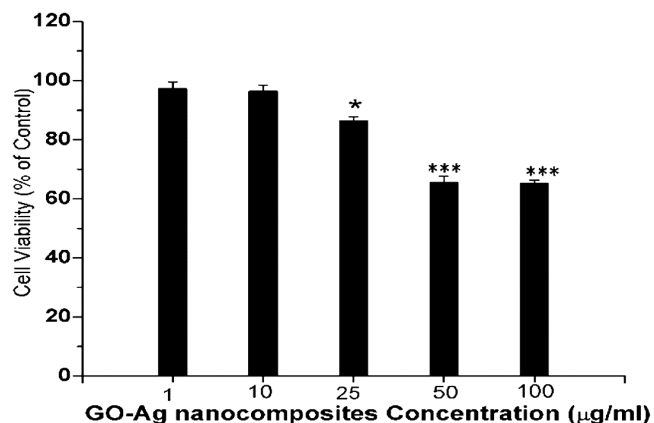


Fig. 5 — Effect of GO-Ag nanocomposites on the cell viability. HepG2 cells were treated with GO-Ag nanocomposites (1, 10, 25, 50 and 100  $\mu\text{g/ml}$ ) for 18 h. Results are expressed as mean  $\pm$  SD,  $n=3$ . \*\*\* $P<0.001$ , \* $P<0.05$  when compared to control.

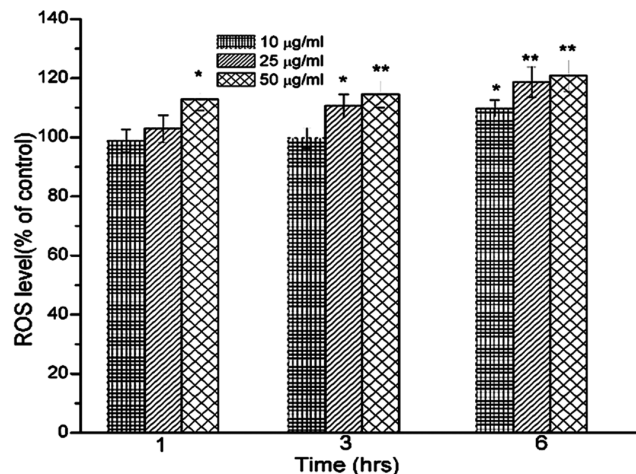


Fig. 6 — Effect of GO-Ag nanocomposites on ROS level. HepG2 cells were treated with GO-Ag nanocomposites (10, 25 and 50  $\mu\text{g/ml}$ ) for 1, 3 and 6 h. Results are expressed as mean  $\pm$  SD,  $n=3$ . \*\* $P<0.01$ , \* $P<0.05$  when compared to control.

### 3.3 Effect of graphene oxide silver nanocomposite on ROS level

Significant enhancement in reactive oxygen species level had been observed at 1 hour with 50  $\mu\text{g/ml}$  concentration of GO-Ag nanocomposites. The rise in ROS level continued and exhibited a significant growth after 3 hours onwards. At 6 hrs, the maximum level of ROS was observed with the concentration of 50 $\mu\text{g/ml}$  (Fig. 6). This result indicated that GO-Ag nanocomposites could induce significant oxidative stress in HepG2 cells which could play a vital role in reducing cell viability.

### 3.4 Effect of graphene oxide silver nanocomposite on glutathione (GSH) level

The results on GSH levels indicated that various concentrations of GO-Ag nanocomposites(10, 25,

Table 1 — Effect of GO-Ag nanocomposite on Glutathione (GSH) levels:

Concentration	GSH Level (% of Control)		
	After 1 hour	After 3hr	After 6hr
10 µg/ml	95.84±0.39	98.45±0.32	87.23±0.45**
25 µg/ml	75.03±0.56***	86.45±0.12**	74.50±0.35***
50 µg/ml	84.0±60.63**	72.83±0.27***	73.64±0.16***

HepG2 cells were treated with GO-Ag nanocomposites (10, 25 and 50 µg/ml) for 1, 3 and 6 h. Results are expressed as mean ± SD. \*\*\*  $p < 0.001$ , \*\*  $p < 0.01$  as compared to control using one-way ANOVA.

Table 2 — Effect of GO-Ag nanocomposite of Caspase-3 activity Groups

Groups	Fluorescence Intensity		
	After 1.5 h	After 3 h	After 6 h
Control	3.12 ± 1.32	3.84 ± 0.96	4.36 ± 1.02
10 µg/ml	3.46±0.85	5.08±0.98	5.11 ± 0.25
25 µg/ml	5.62±1.14	12.62±2.8**	15.24 ± 0.34**
50 µg/ml	10.26±1.26**	20.21±1.84***	21.42±1.54***

HepG2 cells were treated with GO-Ag nanocomposites (10, 25 and 50 µg/ml) for 1.5, 3 and 6 h. Results are expressed as mean ± SD. \*\*\*  $p < 0.001$ , \*\*  $p < 0.01$  as compared to control using one-way ANOVA.

50 µg/ml) caused time-dependent decrease in GSH up to 6 hours. The highest depletion of GSH had been observed at 6 hours with 25µg/ml concentration. As GSH levels decreased in oxidative stress, thus, this result also confirmed the induction of oxidative stress in Hep G2 cells in the presence of GO-Ag nanocomposites (Table 1).

### 3.5 Effect of graphene oxide silver nanocomposite on caspase-3 activity

Caspases are the proteases that cleave certain proteins at the cellular level which can lead cell apoptosis. The GO-Ag nanocomposites had significantly increased the AFC fluorescence in HepG2 cells which specified the increase in caspase-3 activity both in concentration and time dependent manner. The significant rise in caspase activity had been observed at 3 hrs and the maximum activity was observed at 6 hrs with the highest concentration i.e. 50 µg/ml. This result suggested that GO-Ag nanocomposites could activate caspase dependent pathway in Hep G2 cells (Table 2).

### 3.6 Effect of graphene oxide silver nanocomposite on sub g1 population

The effect of GO-Ag nanocomposites on the cell cycle study was observed by cell cycle study using Flow cytometry. The results depicted that there was a significant increase in apoptotic cell population in Hep G2 cells in the presence of 25 and 50 µg/ml concentrations of GO-Ag nanocomposites at 18 hrs.

Table 3 — Modulation of cell death in the presence of antioxidant and caspase inhibitor

Inhibitors	GO-Ag	GO-Ag
	nanocomposite (50µM)	nanocomposite (50µM)
None	100 ± 1.6	69.1 ± 3.2**
NAC (antioxidant)	96.3 ± 2.6	89.8 ± 1.8 <sup>b</sup>
Z-VAD-fmk (caspase inhibitor)	97.5 ± 2.4	87.4 ± 2.6 <sup>b</sup>

HepG2 cells ( $1 \times 10^4$ ) were pre-treated with NAC (10 mM) for 10 mins and Z-VAD-fmk (20 µM) for 1 h, and then with GO-Ag nanocomposite (50µM) for 18 h at 37°C. Absorbance was measured at 530 nm. The data represents mean ± SD. \*\*  $p < 0.01$  as compared to control and <sup>b</sup> $p < 0.05$  as compared to the GO-Ag nanocomposite group, using one-way ANOVA.

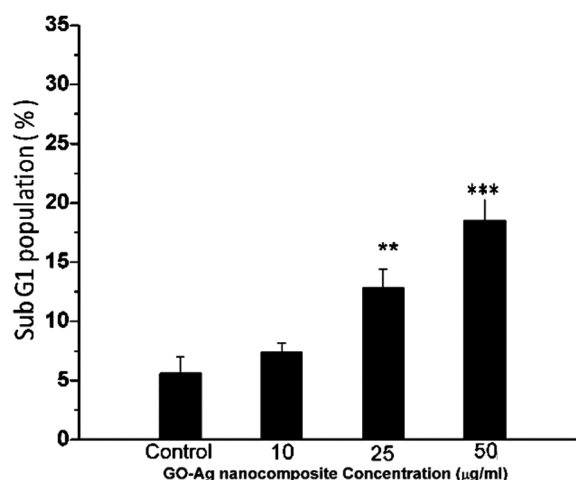


Fig. 7 — Effect of GO-Ag nanocomposites on the cell cycle. HepG2 cells were treated with GO-Ag nanocomposites (10, 25 & 50 µg/ml) for 18 h. Results are expressed as mean ± SD, n=3. \*\*\* $P < 0.001$ , \*\* $P < 0.01$  when compared to control.

The cell cycle result confirmed the induction of apoptotic cell death in Hep G2 cells by GO-Ag nanocomposites (Fig. 7).

### 3.7 Effect of Inhibitors on Cell death

The results on ROS level, GSH level and caspase activity suggested the involvement of oxidative stress and caspases in GO-Ag nanocomposites induced apoptotic cell death in cancer cells. These results were further confirmed by adding the inhibitors i.e. thiol antioxidant (N-acetyl cysteine, NAC) and general caspase inhibitor (Z-VAD-fmk)<sup>25</sup>. The pre-treatment of NAC, which raised intracellular GSH level and protected the cell from the ROS effects, had significantly restored the GO-Ag nanocomposites induced apoptotic cell death (Table 3). This result confirmed the role of oxidative stress in GO-Ag nanocomposites induced cell death in Hep G2 cells. The presence of caspase inhibitor had also prevented the apoptotic cell death up to significant extent. These

results confirmed the role of oxidative stress and caspases in GO-Ag nanocomposites induced apoptosis.

#### 4 Conclusion

In the present investigation, the effect of GO-Ag nanocomposites in human hepatoma cells (HepG2) has been observed. Results clearly demonstrate that different concentrations of GO-Ag nanocomposites can significantly induce cytotoxicity, apoptosis and oxidative stress in HepG2 cells. The significant cell death has been observed in HepG2 cells at low molar concentration (25  $\mu$ M). The nanocomposites significantly increased the ROS level and depleted GSH levels in concentration- as well as time-dependent manner. ROS and GSH are the oxidative stress markers indicating the induction of oxidative stress by nanocomposites. ROS, act as intracellular signal prior to mitochondrial membrane depolarization and caspase-3 activation. The apoptotic marker i.e. caspase-3 activity has also increased, which plays an important role in apoptotic pathway. The sub G1 population analysis by cell cycle study demonstrates a significant increase in apoptotic DNA in the presence of GO-Ag nanocomposites. These results strongly indicate GO-Ag nanocomposites induced apoptotic cell death in HepG2 cells. Further, the pre-treatment of inhibitors confirms the significant role of oxidative stress in GO-Ag nanocomposites induced apoptosis through caspase-dependent pathway.

It seems that the different intracellular parameters studied in this investigation, such as ROS and GSH preceding caspase-3 activation followed by DNA damage at 18 hr, are all interrelated and any change in early signals may ultimately lead to changed apoptosis. In conclusion, this study clearly demonstrate that GO-Ag nanocomposites induce cytotoxicity, oxidative stress and apoptosis in HepG2 cells through caspase dependent pathway. Although, the possibility of caspase-independent pathway also exists which requires further detailed investigation to provide a better understanding of the mechanism.

#### Acknowledgement

The authors are thankful to Central Instrumentation Facility, BIT Mesra from where they availed all the characterization facilities.

#### References

- 1 Al-Ani L A, Yehye W A, Kadir F A, Hashim N M, AlSaadi M A & Julkapli N M, *PLoS One*, 14 (2019) e0216725.
- 2 Chakraborty N, Sharma R, Singh R K, Mukherjee, S K & Sharma N, *NANO*, 17 (2022) 2250115.
- 3 Vi T, Kumar S R, Rout B, Liu C H, Wong C B & Chang C W, *Nanomater*, 8 (2018) 163.
- 4 Sharma N, Bhattacharjee R & Sharma R, *Acta Microbiol Bul*, 37 (2021) 195.
- 5 Singh D, Singh M, Yadav E, Falls N, Komal U & Dangi D S, *RSC Adv*, 8 (2018) 6940.
- 6 Zhao X, Chen Q, Liu W, Li Y, Tang H & Liu X, *Int J Nanomed*, 10 (2014) 257.
- 7 Guo Z, Zhou Y, Yang J & Shao X, *Biomed Pharmacother*, 110 (2019) 371.
- 8 Zhu D, Tao W, Zhang H, Liu G, Wang T & Zhang L, *Acta Biomater*, 30 (2016) 144.
- 9 Raza A & Sood G K, *World J Gastroenterol*, 20 (2014) 4115.
- 10 Bajpai A & Sharma R, *Vacuum*, 172 (2020) 109033.
- 11 Ravanshad R, Karimi Zadeh A, Amani A M, Mousavi S M, Hashemi S A & Savar Dashtaki A, *Nano Rev Exp*, 9 (2018) 1373551.
- 12 Zaaba N I, Foo K L, Hashim U, Tan S J, Liu W W & Voon C H, *Procedia Eng*, 184 (2017) 469.
- 13 Zheng H, Ni D, Yu Z & Liang P, *Food Chem*, 217 (2017) 511.
- 14 Kumar A, Sasmal D & Sharma N, *Environ Toxicol Pharmacol*, 39 (2015) 504.
- 15 Kumar A, Sharma R, Rana D & Sharma N, *Endo Metabol Immune Dis - Drug Tar*, 19(2019) 171.
- 16 Kumar A, Sasmal D & Sharma N, *J Appl Toxicol*, 34 (2014) 1303.
- 17 Kumar A & Sharma N, *Pestic Biochem Physiol*, 119 (2015) 16.
- 18 Kumar A, Sasmal D, Bhaskar A, Mukhopadhyay K, Thakur A & Sharma N, *Environ Toxicol*, 31 (2016) 808.
- 19 Ryu S H & Shanmugaraj A M, *Chem Eng J*, 244 (2014) 552.
- 20 Cao N & Zhang Y, *J Nanomater*, 2015 (2015) 1.
- 21 Khorrami S, Abdollahi Z, Eshaghi G, Khosravi A, Bidram E & Zarrabi A, *Sci Rep*, 9 (2019) 1.
- 22 Amit K & Sharma R, *Surf Rev Lett*, 25 (2018) 1850055.
- 23 Kumari S, Sharma P, Yadav S, Kumar J, Vij A, Rawat P & Kumar S, *ACS Omega*, 5 (2020) 5041.
- 24 Chakravarty M, Sharma R, Amit K, Sharma N & Pradhan S K, *Int J Nanosci*, 15 (2016) 1660016.
- 25 Sharma N, Banerjee S & Mazumder P M, *Pestic Biochem Physiol*, 149 (2018) 98.